JOURNAL OF ENGINEERING annals OF FACULTY OF ENGINEERING HUNEDOARA

INVESTIGATION INTO EXTRUSION OF SINTERED PREFORM FLOW

[1]Abhay Kumar SHARMA, [2]R.K. RANJAN, [3]K.S. KASNAM, [4]V.K. BAJPAI

[1-2]Mechanical Engineering Department, BRCM College of Engineering & Technology Bahal, INDIA
[3-4]Mechanical Engineering Department, NIT Krukshetra (Institute of National Importance), INDIA

Abstract
The forming of sintered metal-powder performs is currently arousing interest in many parts of the world as an economic method of producing components from metal powders. This paper reports on an investigation into the various aspects of extrusion of powder preforms, which have been compacted and sintered from atomized powder. An attempt has been made for the determination of the die pressures developed during the extrusion of powder preform by using an upper bound approach. The concept of a spherical velocity field is introduced and dealt with in great detail, and the power required. Experiments were conducted on aluminum and copper metal powder performs to validate the theoretical results. The results so obtained are discussed critically to illustrate the interaction of various process parameters involved and are presented graphically.
Keywords: Preforms, sintering, conical converging die, inter facial friction law

1. INTRODUCTION

During the last few years metal-powder components have assumed an important position in industry, as they are being used successfully in a wide range of applications. Both the mechanical and the metallurgical properties of the metal powder components compare favorably with those of wrought materials[1]. Bulk processing of metal powder preforms is a convenient method of reducing or eliminating the porosity from the conventional powder metallurgy products. Process is attractive because it avoids large number of operations, high scrap losses and high-energy consumption associated with the conventional manufacturing processes such as casting, machining etc. In this new technology sintered porous powder preforms are used as starting materials in metal forming processes. Metal powder products manufactured by this new technology are comparable and in some cases even superior to those of cast and wrought products.

Although a considerable amount of work has been reported recently as the various technological aspects of the industrial processing of metal-powder preforms[2-4], no systematic attempt has been made so far to study the processing load and deformation characteristics during flow through conical converging dies.

The paper reports on an investigation into the various aspects of extrusion of powder preforms, which have been compacted and sintered from atomized powder. An attempt has been made for the determination of the die pressures developed during the extrusion of powder preform by using an upper bound approach. The concept of a spherical velocity field is introduced and dealt with in great detail, and the power required. The results so obtained are discussed critically to illustrate the interaction of various process parameters involved and are presented graphically.

It is expected that the present work will be of great importance for the assessment of relative extrusion stress developed during the flow through conical converging dies of metal powder preforms.

2. INTERFACIAL FRICTION LAW

In an investigation of the plastic deformation of metal-powder preforms, it is evident that with the application of compressive hydrostatic stress the pores will close and the relative density will increase, whereas the application of tensile hydrostatic stress the pores will grow and the relative density will decrease. The density distribution also does not seem to be uniform throughout, being high in the central region and low at the edges. The density distribution will be more uniform for smaller coefficient of friction μ and for a greater initial density[5].

During the forming of metal-powder preforms the compressive force gradually increases the relative density, which later is directly proportional to the real area of contact. The relative density gradually approaches the apparent relative density (Fig.1) this approach probably being asymptotic[6].

Friction condition between deforming tool and work piece in metal forming are of the greatest importance concerning a number of factors such as force and mode of deformation, properties of the finished specimen and resulting surface roughness. During the sinter forging process it is very important to keep special consideration on the interfacial friction, as this will determine the success or failure of the operation. The relative velocity between the work piece material and the die surface, together with high interfacial pressure and or deformation modes, create a condition of composite friction which is due to adhesion and sliding[7]. The shear equation becomes $\tau = \mu\lfloor p + \rho_0 \phi_0 \rfloor$. The first term μp being due to sliding and second term $\mu\rho_0\phi_0$ being due to adhesion, which later arises from change of the relative density of the preform during the process.

The pattern of the metal flow during the forging of a metal powder preform is such that there exists two zones, an inner one where no relative movement between work piece and die occurs (the sticking zone) and an outer zone where sliding occurs. Therefore, the appropriate friction law for particular condition is:

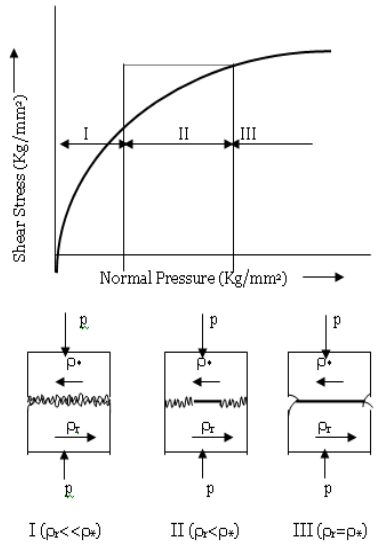

Fig. 1 Three regimes of density variation

$$\tau = \mu\left[p + \rho_0 \phi_0 \left\{ 1 - \frac{r}{nR} \right\} \right] \quad (1)$$

where r denotes the sticking zone radius & which may be approximated by the relation given by Rooks[8] and n>>1.

3. PLASTIC DEFORMATION OF SINTERED PREFORM

In an investigation of the plastic deformation of sintered deformation of sintered metal powder preforms it is clear that change in volume occurs due to porosity. A preform with a high relative density yields at a relative high stress whereas a low relative density preform yields at a relatively low stress. Even hydrostatic stress can cause the sintered metal powder preforms to yield, as the yield surface is closed on the hydrostatic stress axis. The density distribution also does not seem to be uniform throughout, being high in the central region and low at the edges. The density distribution will be more uniform for a smaller coefficient of friction and for a higher initial-density preform.

Tabata and Masaki[9] proposed the following yield criterion for porous metal powder preforms:

$$\rho^k = \sqrt{3J_2'} \pm 3\eta\sigma_m \quad (2)$$

The negative sign is taken for $\sigma_m \le 0$ and the positive sign is taken for $\sigma_m > 0$.

The values of η and k were determined experimentally from simple compression and tension test of sintered copper-powder preforms[9] as

$$\eta = 0.54(1-\rho)^{1.2} \text{ for } \sigma_m \le 0$$

$$\eta = 0.55(1-\rho)^{0.83} \text{ for } \sigma_m > 0 \text{ and } k=2$$

For the axisymmetric condition the yield criterion reduces to

$$\sigma_1 - \sigma_2 = \frac{\rho^k \sigma_0}{(1-2\eta)} + \frac{(1+\eta)}{(1-2\eta)}\sigma_2 - \sigma_2 = \lambda \text{ (Say)} \quad \text{(Appendix A)} \quad (3)$$

4. SPHERICAL VELOCITY FIELD

The wire is divided into three regions in which the velocity fields are continuous (Fig. 2). In zone-I and zone-III, the velocity is uniform and has only an axial component. In zone-I, the velocity is v_0, and in zone-III the velocity is v_f.

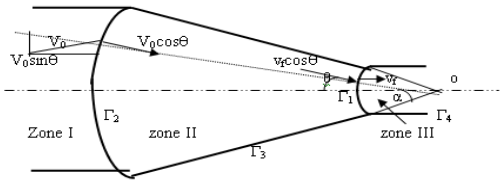

Fig. 2 The spherical velocity field

Because of mass constancy

$$v_0 = \rho v_f \left(\frac{R_f}{R_0} \right)^2 \quad (4)$$

In zone-I, deformation has not yet begun. It consists of the incoming rod, which is separated from the deforming zone-II by the surface Γ_1. Surface Γ_2 is spherical, of radius r_0 with the origin at the apex– o of

the cone of the die. Zone-II is the zone of deformation bounded by the surface of the die, with a cone of an included angle 2α and two concentric spherical surfaces Γ_1 and Γ_2. The surface Γ_2 is the spherical boundary between zone-I and II. The spherical surface Γ_1 of radius r_f, with the origin at the apex –O of the cone, separates zone-II from the emerging product of zone-III. In zone-II, the velocity is directed towards the apex –O of the cone, with cylindrical symmetry.

In the spherical co-ordinate system (r, θ, φ), the velocity components are

$$U_r = -\frac{v_f\, r_f^2 \cos\theta}{r^{1/K}};\quad U_\theta = 0;\quad U_\varphi \tag{5}$$

where $K = \dfrac{(1-2\eta)}{2(1+\eta)}$

5. STRAIN RATE

$$\dot{\varepsilon}_r = \frac{v_f\, r_f^2 \cos\theta}{K\, r^{(1/K)+1}};\ \dot{\varepsilon}_\theta = -\frac{v_f\, r_f^2 \cos\theta}{K\, r^{(1/K)+1}};\ \dot{\varepsilon}_\varphi = -\frac{v_f\, r_f^2 \cos\theta}{K\, r^{(1/K)+1}};\quad \dot{\varepsilon}_{r\theta} = \frac{v_f\, r_f^2 \sin\theta}{2\, r^{(1/K)+1}} \tag{6}$$

The above strain rates must satisfy the compressibility equation of powder preform[9]-

$$\left(\dot{\varepsilon}_r + \dot{\varepsilon}_\theta + \dot{\varepsilon}_\varphi\right) = \sqrt{2}\eta\sqrt{\left(\dot{\varepsilon}_r - \dot{\varepsilon}_\theta\right)^2 + \left(\dot{\varepsilon}_\theta - \dot{\varepsilon}_\varphi\right)^2 + \left(\dot{\varepsilon}_\varphi - \dot{\varepsilon}_r\right)^2} \tag{7}$$

This equation may be rewrite as according to our problem:

$$\dot{\varepsilon}_r + \frac{2(1+\eta)}{(1-2\eta)}\frac{U_r}{r} = 0 \tag{8}$$

6. INTERNAL POWER OF DEFORMATION

According to Oyane & Tabata[10], the internal work done is given by-

$$W_i = \frac{2}{\sqrt{3}}\rho^k\sigma_0 \int_V \left[\frac{1}{2}\left(\dot{\varepsilon}_r^2 + \dot{\varepsilon}_\theta^2 + \dot{\varepsilon}_z^2 + 2\dot{\varepsilon}_{r\theta}^2\right)\right]^{\frac{1}{2}} dV \tag{9}$$

$$= \frac{\sqrt{2}}{\sqrt{3}}\rho^k\sigma_0 \int_V \sqrt{\left[\frac{v_f\, v_f^2 \cos^2\theta}{r^{2\{(1/K)+1\}}}\left\{\frac{1}{K^2}+2\right\} + \frac{v_f^2 r_f^4 \sin^2\theta}{2\, r^{2\{(1/K)+1\}}}\right]} dV$$

and $dV = 2\pi r \sin\theta . r d\theta . dr$

$$= \frac{2\sqrt{2}}{\sqrt{3}}\pi\rho^k\sigma_0 v_f r_f^2 \int_0^\alpha \int_{r_f}^{r_0} \sqrt{\left[\left\{\left(\frac{1}{K^2}+2\right)\cos^2\theta + \frac{\sin^2\theta}{2}\right\}\frac{1}{r^{2\{(1/K)+1\}}}\right]} r^2 \sin\theta . d\theta . dr$$

$$= \frac{\sqrt{2}\pi\rho^k\sigma_0\sqrt{1+2K^2}\, v_f\, r_f^2\left(r_0^{2-1/K} - r_f^{2-1/K}\right)}{\sqrt{3}(2K-1)} \left[1 - \cos\alpha\sqrt{1 - \frac{2+3K^2}{2(1+2K^2)}\sin^2\alpha} + \frac{1 - \frac{2+3K^2}{2(1+2K^2)}}{\sqrt{\frac{2+3K^2}{2(1+2K^2)}}} \ln \frac{1 + \frac{2+3K^2}{2(1+2K^2)}}{\sqrt{\frac{2+3K^2}{2(1+2K^2)}} + \sqrt{1 - \frac{2+3K^2}{2(1+2K^2)}\sin^2\alpha}}\right]$$

Since $\frac{r_0}{r_f}=\frac{R_0}{R_f}$ and $r_f=\frac{R_f}{\sin\alpha}$; it follows that:

$$W_i=\frac{\sqrt{2}\pi\rho^k\sigma_0\sqrt{1+2k^2}\,v_f\,r_f^{(4-1/K)}}{\sqrt{3}(2K-1)}\left[\left(\frac{R_o}{R_f}\right)^{2-\frac{1}{K}}-1\right].f(\alpha)$$

$$f(\alpha)=\frac{1}{\sin^{(4-1/K)}\alpha}\left[1-\cos\alpha\sqrt{1-\frac{2+3K^2}{2(1+2K^2)}\sin^2\alpha}+\frac{1-\frac{2+3K^2}{2(1+2K^2)}}{\sqrt{\frac{2+3K^2}{2(1+2K^2)}}}\ln\frac{1+\frac{2+3K^2}{2(1+2K^2)}}{\sqrt{\frac{2+3K^2}{2(1+2K^2)}}+\sqrt{1-\frac{2+3K^2}{2(1+2K^2)}\sin^2\alpha}}\right]$$

For very small α, f (α) converges to unity and equation () reduces to-

$$W_i=\frac{\sqrt{2}\pi\rho^k\sigma_0\sqrt{1+2K^2}\,v_f\,r_f^{(4-1/K)}}{\sqrt{3}(2K-1)}\left[\left(\frac{R_o}{R_f}\right)^{2-\frac{1}{K}}-1\right].f(\alpha) \qquad (10)$$

7. VELOCITY DISCONTINUITIES

along Γ_1- $\Delta v=v_f\sin\theta$

along Γ_2- $\Delta v=v_0\sin\theta$

along Γ_3- $\Delta v=\frac{v_f\,r_f^2\cos\alpha}{r^{1/K}}\approx\frac{v_f\,R_f^2\cos\alpha}{R^{1/K}}$

along Γ_4- $\Delta v=v_f$ (11)

8. FRICTIONAL POWER LOSSES

In Cylindrical Portion

Consider the equilibrium of the small element (Fig.3):

$$(\sigma_x+d\sigma_x)\pi R_0^2-\sigma_x\pi R_0^2-2\mu p\pi R_0\,dx=0 \qquad (12)$$

For cylindrical state of stress, the principal stresses are σ_r, σ_θ and σ_z. Hence, equation (3) becomes

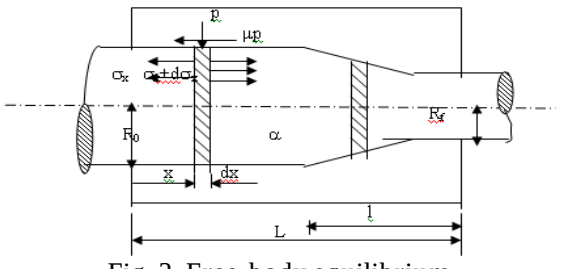

Fig. 3 Free-body equilibrium

$$\sigma_r-\sigma_\theta=\frac{\rho^k\sigma_0}{(1-2\eta)}+\frac{(1+\eta)}{(1-2\eta)}\sigma_\theta-\sigma_\theta=\lambda \text{ (Say)}$$

As the yielding of the material during this process takes place at a particular maximum value of σ_θ. Hence λ is a constant for this process (Appendix A) when $\sigma_r=\sigma_x$, and $\sigma_\theta=-p$.

Von Mises yield criteria reduces to:

$$\sigma_x+p=-\lambda;\qquad \text{i.e. } p=-(\sigma_x+\lambda) \qquad (13)$$

$$\Rightarrow\frac{R_0}{2}d\sigma_x=\mu p\,dx=-\mu(\sigma_x+\lambda)dx\Rightarrow\frac{d\sigma_x}{(\lambda+\sigma_x)}=-2\frac{\mu}{R_0}dx$$

and by integration, $\ln(\lambda+\sigma_x)=-2\frac{\mu}{R_0}x+C$

Using boundary condition, $\sigma_x=\sigma_{xb}$ at x = 0. Now, $C=\ln(\lambda+\sigma_{xb})$

After putting the value of C in the above equation, we get,

$$\sigma_x = \lambda\left[\left(1+\frac{\sigma_{xb}}{\lambda}\right)\exp\left(-2\mu\frac{x}{R_0}\right)-1\right] \tag{14}$$

Now, $p = -(\lambda+\sigma_x) = -\lambda\left(1+\frac{\sigma_{xb}}{\lambda}\right)\exp\left(-2\frac{\mu}{R_0}x\right)$

$$W_f = \int_s \tau|\Delta v|ds \tag{15}$$

$$W_f = 2\pi v_f R_f^2\frac{\mu}{R_0}\int_{x=0}^{L-l} p\,dx; \Rightarrow -2\pi v_f R_f^2\frac{\mu}{R_0}\lambda\left(1+\frac{\sigma_{xb}}{\lambda}\right)\int_{x=0}^{L-l}\exp\left(-2\frac{\mu x}{R_0}\right)dx$$

After integrating and substituting, $l = (R_0 - R_f)\cot\alpha$

$$W_f = \pi v_f R_f^2\lambda\left(1+\frac{\sigma_{xb}}{\lambda}\right)\left|\exp\left[-2\mu\left\{\frac{L}{R_0}-\left(1-\frac{R_f}{R_0}\right)\cot\alpha\right\}\right]-1\right| \tag{16}$$

In Conical Portion

The die and differential element are shown in Fig. 3. Considering the equilibrium of the forces in x-direction which is the direction of principal stress,

$$Dd\sigma_x + 2\sigma_x dD + 2dD\left(p+\frac{\tau}{\sin\alpha}\right) = 0$$

or, $Dd\sigma_x + 2\sigma_x dD + 2dD\left\langle p+\left(\frac{\mu}{\tan\alpha}\right)\left[p+\rho_0\phi_0\left\{1-\left(\frac{r}{R_b}\right)\frac{1}{n}\right\}\right]\right\rangle$

After simplifying of the above equation, we get,

$$Dd\sigma_x + 2dD\left\langle(\sigma_x+p)+B\left[p+\rho_0\phi_0\left\{1-\left(\frac{D}{D_b}\right)\frac{1}{n}\right\}\right]\right\rangle = 0 \tag{17}$$

where $B = \frac{\mu}{\tan\alpha}$

Equation (17) reduces to,

$$Dd\sigma_x + 2dD\left\langle\lambda(1+B)-B\left[\sigma_x-\rho_0\phi_0\left\{1-\left(\frac{D}{D_b}\right)\frac{1}{n}\right\}\right]\right\rangle = 0 \tag{18}$$

Integrating and simplifying the equation (18),

$$\sigma_x = \frac{2B\rho_0\phi_0}{n(D/D_b)}\cdot\frac{1}{(1-2B)}+\frac{1}{2B}\left[2\lambda(1+B)+2B\rho_0\phi_0\right]+CD^{2B} \tag{19}$$

Using boundary condition at entry for this case is,

$$\sigma_x = \sigma_{xf} \qquad \text{at } D = D_f$$

Using this value in equation (19)-

$$C = D_f^{-2B}\left[\sigma_{xf}-\frac{1}{B}\left\{\lambda(1+B)+B\rho_0\phi_0\right\}-\frac{2B\rho_0\phi_0}{(1-2B)n}\right] \tag{20}$$

Substituting the value of C in equation (19) and after simplification without considering front pressure, we can get,

$$\frac{\sigma_x}{\lambda} = \frac{1+B}{B}\left[1-\left(\frac{D}{D_f}\right)^{2B}\right]+\frac{\rho_0\phi_0}{\lambda}\left[1-\left(\frac{D}{D_f}\right)^{2B}\left\{1+\frac{2B}{n(1-2B)}\frac{D_f}{D_b}\right\}+\frac{2B}{n(1-2B)}\frac{D}{D_b}\right] \tag{21}$$

Now from equation (15), we can get,

$$W_f = 2\pi\lambda v_f R_f^2 \cot\alpha \int_{R_f}^{R_0} \left\langle \frac{1-\frac{1+B}{B}\left\{1-\left(\frac{D}{D_f}\right)^{2B}\right\}-\frac{\rho_0\phi_0}{\lambda}\times}{\left[1-\left(\frac{D}{D_f}\right)^{2B}\left\{1+\frac{2B}{n(1-2B)}\frac{D_f}{D_b}\right\}+\frac{2B}{n(1-2B)}\frac{D}{D_b}\right]} \right\rangle R^{1-1/K}.dR$$

$$W_f = \frac{2\pi v_f R_f^2 \cot\alpha.\lambda K R_f^{(2-1/K)}}{(2K-1)}\left[\left(\frac{R_0}{R_f}\right)^{(2-1/K)}-1\right]\times$$

$$\left[\begin{array}{l} 1-\frac{1+B}{B}\left\{1-\left|\left(\frac{R_0}{R_f}\right)^{2B}-1\right|\frac{2K-1}{2BK+2K-1}\right\} \\ -\frac{\rho_0\phi_0}{\lambda}\left|\begin{array}{l} 1-\left\{\left(\frac{R_0}{R_f}\right)^{2B}-1\right\}\frac{2K-1}{2BK+2K-1}\left\{1+\frac{2B}{n(1-2B)}\frac{R_f}{R_0}\right\} \\ +\frac{2B}{(1-2B)}\left(1-\frac{R_f}{R_0}\right)\left(\frac{2K-1}{3K-1}\right) \end{array}\right| \end{array}\right] \quad (22)$$

9. RELATIVE EXTRUSION PRESSURE

The total power required for the process can be split up into parts:

(a) The power loss due to shear at surface of velocity discontinuities Γ_1 and Γ_2 .
(b) The internal loss due to friction along die surfaces Γ_3 and Γ_4.
(c) The internal work of deformation.

For plastic deformation of a metal powder the external power $\overset{*}{J}$ supplied by the ram is given as:

$$\overset{*}{J} = W_i + W_f + W_a + W_t \quad (23)$$

The first term on the right hand side denotes the rate of internal energy dissipation W_i, the second term denotes the frictional shear energy losses W_f, the third term denotes the energy dissipation due to inertia forces W_a, and the last term covers power supplied by predetermined body tractions W_t. In this case a force due to inertia is negligibly small and no external surface traction is stipulated. Therefore, $W_a = W_t = 0$.

Now the external power $\overset{*}{J}$ supplied by the press through the platen is –

$$\overset{*}{J} = \int F_i U_i ds = = W_i + W_f \quad (24)$$

and $\overset{*}{J} = -\pi\rho v_f R_f^2 \sigma_{xb}$ (25)

10. RESULTS AND DISCUSSION

Fig. 4(a) shows the physical model of deformation of a metal powder preform through a conical converging die. During the process of deformation of metal powder preform, it is seen that initially the densification of particles take place and thus the density of the preform increases gradually. The applied stress has more contribution towards densification (compaction) and less contribution towards compression. After attaining sufficient density the densification and compression take place simultaneously. The applied stress now contributes more towards compression and less towards densification. However, the extent of each of them depends upon the reduction ratio and the initial relative density of the preform. When a further deformation stress is applied, the stress-free portion is completely deformed and replaced by densified material. The later starts to emerge from the die orifice, while the elastically deformed part of the preform crosses the back boundaries of the plastically deformed zone and starts a process of densification and this continues until the whole preform is

deformed. Fig. 4(b) shows the effect of semi cone angle (α) of the die. It is found that with the increase of semi cone angle (α) of the die, the deformation stress decreases.

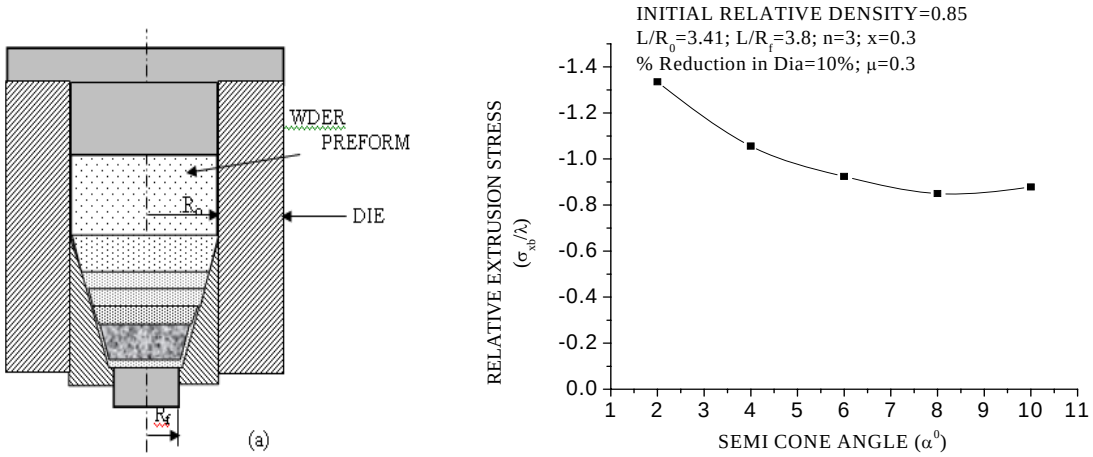

FIG. 4 (a) Physical model of deformation of a metal powder preform through a conical converging die (b) effect of semi cone angle (α) on relative extrusion pressure

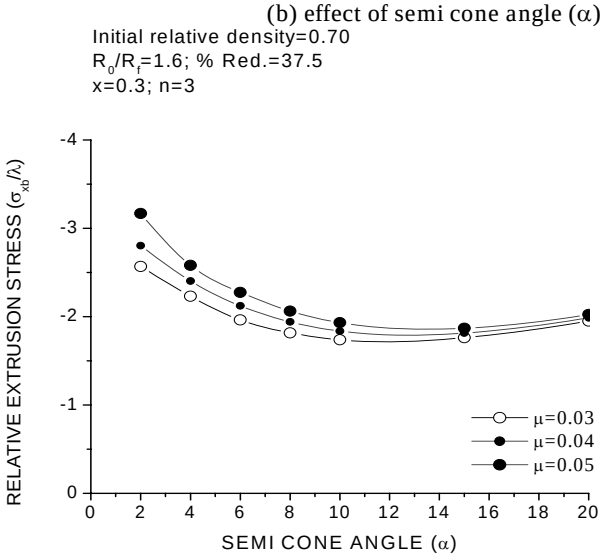

FIG. 5. Variation of theoretical relative extrusion stress with semi cone angle at different coefficient of friction

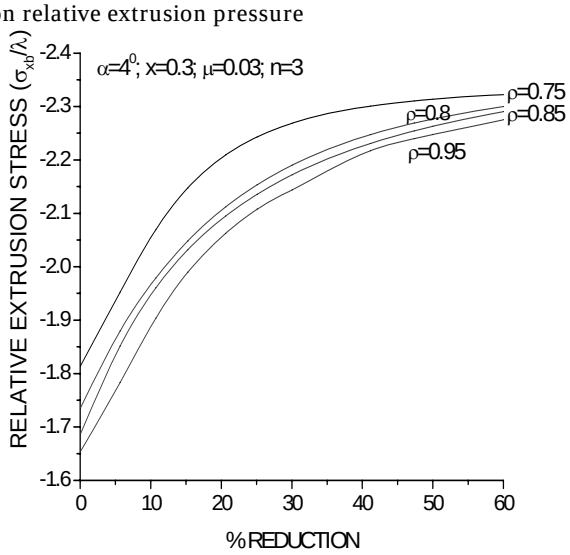

FIG. 6. Variation of relative extrusion stress with percentage reduction in diameter at different initial relative density of the preform

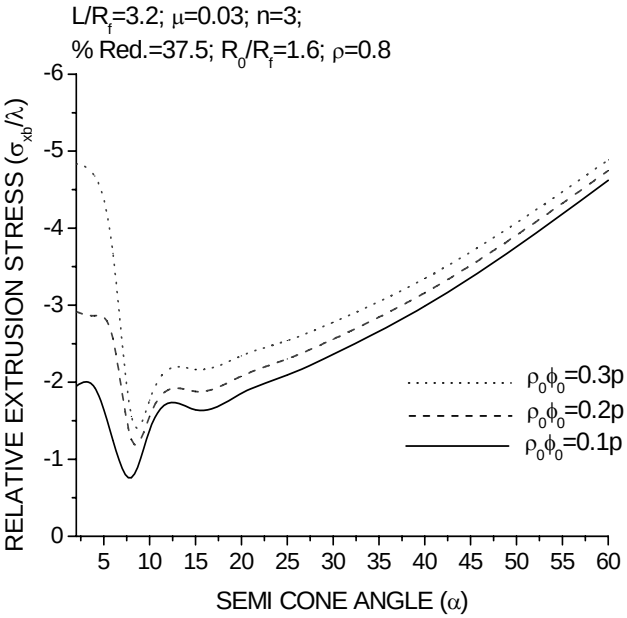

FIG. 7. Variation of theoretical relative extrusion stress with semi cone angle at different value of $\rho_0\phi_0$

Fig. 5 shows the variation of theoretical relative extrusion stress with semi cone angle considering different value of coefficient of friction. The relative extrusion stress increases with increasing the coefficient of friction between preform and die wall.

Fig. 6 shows the variation of theoretical relative extrusion stress with percentage reduction in diameter (reduction ratio) of the preform. For lower value of percentage reduction in diameter, relative extrusion stress varies linearly. As relative density increases relative extrusion stress decreases. Fig. 7 shows the effect of density factor $\rho_0\phi_0$ on the deformation stress for the case of deformation through conical converging dies. With the increase of density factor $\rho_0\phi_0$, the deformation stress increases.

In order to study the deformation characteristics, cylindrical Aluminium and copper billets were pushed through conical converging dies. The dies are given 2^0, 4^0 ,6^0 and 10^0 semi cone angles. The dies gave reductions ratios 1.6, 3.8, 4.2 and 10. The experiments were conducted both at slow and at high speed for different semi cone angles of die and different reductions ratios. Five Aluminium and Copper preforms of different length having initial relative density of 0.85 were taken. The extrusion dies made for the sintered preform has been shown in the Fig. F-1. Fig. F-2 shows the sintered Al preform.

F-1. Conical converging die arrangements

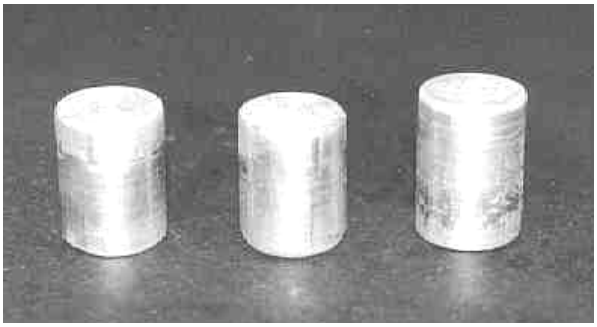

F-2. Sintered Aluminium Powder Preforms

a.

b.

F- 3. Extruded al preform (length of preform=2.63cm; die angle=6^0, reduction ratio=1.6)

F-4. Extruded copper preform (semi cone angle of the die=6^0, reduction ratio=1.6)

Fig. 9 shows the variation of deformation compressive load with percentage reduction in diameter for Aluminium and Copper powder preform having initial relative density equal to 0.85. Deformation load increases with percentage reduction in the diameter of the preform. Initially large amount of compressive load is consumed in compaction of the preform and hence shows a linear variation with large slope. After attaining the sufficient densification, the preform gets deformed plastically and hence shows the variation of curve nearly asymptotic.

Fig. F-3(a) shows a snap for extruded sintered Al powder preform of length 2.63 cm through 4^0 semi cone angle die. Fig. F-3(b) shows extruded Al billet cut into three pieces. F-4 shows extruded copper preform through 6^0 semi cone angle die and reduction ratio equals to 1.6.

Fig. 8 shows the variation of relative extrusion stress containing theoretical as well as experimental results on Aluminium preform having initial relative density equals to 0.85. Figure shows the close agreement between theoretical and experimental results.

ALUMINIUM PREFORM
INITIAL RELATIVE DENSITY = 0.85
μ=0.3; $\alpha=4^0$; n=3; x=0.3

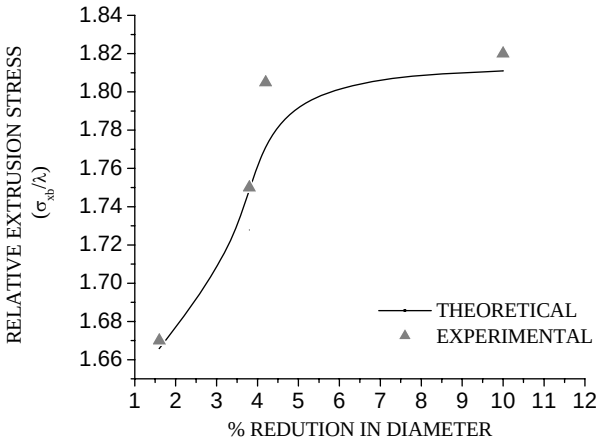

FIG. 8. Variation of relative extrusion stress with percentage reduction in diameter of the aluminium powder preform (Size of the preform: ϕ1.48x2.63cm)

Fig. 10 shows the load-displacement curve for Aluminium and Copper powder preform having initial relative density equal to 0.85 of length 2.0 cm, 2.63 cm and 3.0 cm each. It has been seen that

slope of the curve for different length of the metal powder preform is nearly same. Initially, the difference between the deformation loads is same. The difference is significant as displacement of punch is more forward. It is due to the change in the length of the preform, and therefore it is due to the change in the friction force between preform and die wall. At the end of the process, the difference between the forces is negligible. As seen from the Fig. 10(a) & 10(b), the deformation load increases rapidly at the start of the operation. After some movement of the punch, the load decreases with a constant slope. Again, two common phenomenon occurs in the deformation of metal powder preform i.e. compaction or densification and plastic deformation. Initially large amount of load is consumed by increasing the density of the preform and after getting sufficient densification, preforms get deformed plastically. At the end of the process lower frictional resistance is found and that's why curve sloping down. This curves also on the effect of length of the metal powder preform. As length of the preform increases, deformation load increases.

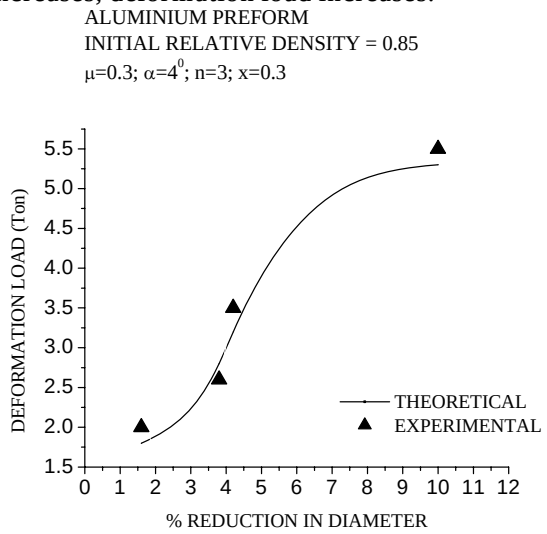

FIG. 9 (a) Variation of deformation load with percentage reduction in the diameter of the preform

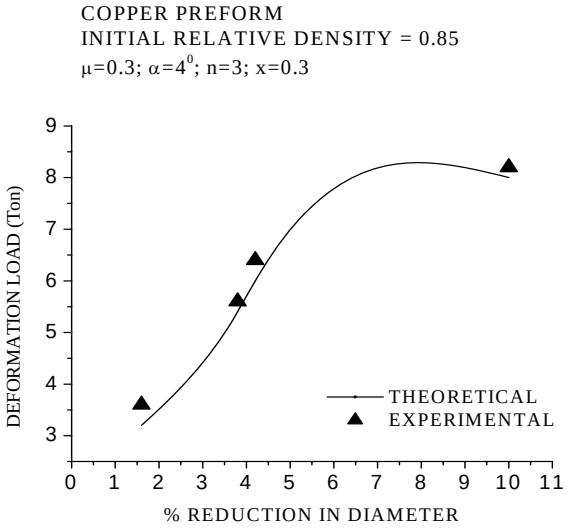

FIG. 9 (b) Variation of deformation load with percentage reduction in the diameter of the preform

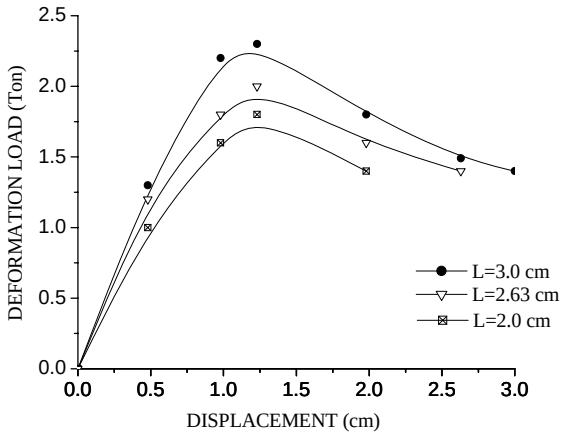

FIG. 10 (a) Load displacement curve of aluminium preform of length: (a) 2.0 cm (b) 2.63 cm (c) 3.0 cm

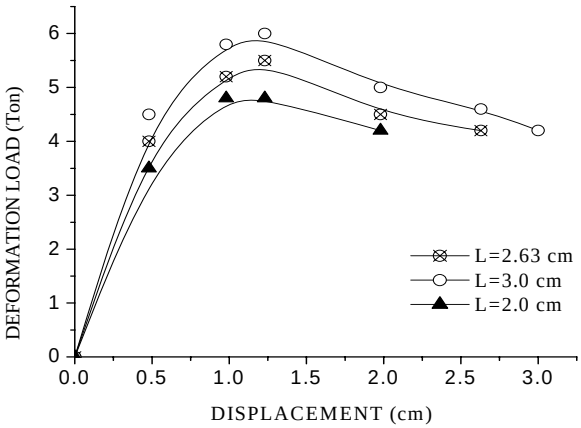

FIG. 10 (b) Load displacement curve of copper preform of length: (a) 2.0 cm (b) 2.63 cm (c) 3.0 cm

Fig. 11 shows the variation of average relative density with reduction ratio for deformation of Aluminium powder performs through conical converging dies. The result shows a tendency for the relative density at slow speed to be slightly higher than at high speed. This is due to the effect of inertia and frictional forces acting during the process. During deformation an important factor, which will affect the relative density of the deformed part, is the effect of speed on the metal flow. The first portion of material to be deformed undergoes a relative small amount of deformation, which means that the material is deformed in a state close to its original form. The amount of flow of this portion of the deformed part depends upon the frictional level, which changes with speed. At high speed friction is decreased, so more deformed metal passes the die in the beginning of deformation that at slow speed.

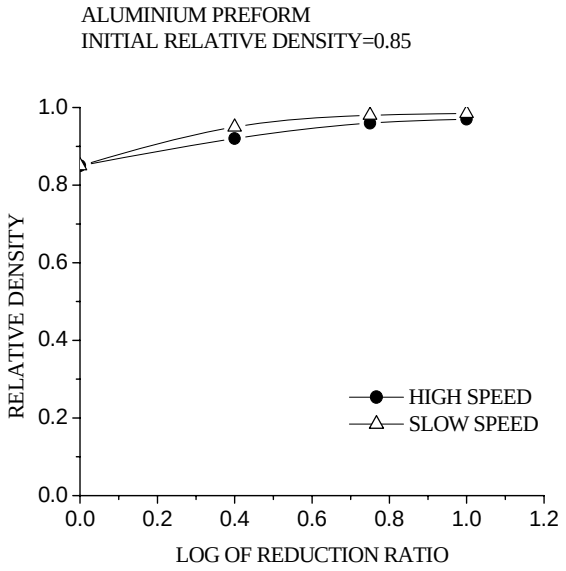

FIG. 11. Variation of relative density (deformed portion) with reduction ratio

11. CONCLUSION

Relative extrusion stress shows minima at a particular semi cone angle of the die, so it can be used criteria for the forming through conical dies. Lower value of coefficient of friction requires low value of relative extrusion stress, i.e. it favors the forming operation. Higher initial relative density of the preform needs lower value of relative extrusion stress. For small semi cone angle, the geometry of the preform doesn't effect too much on the relative extrusion stress. So all the above conclusions certainly would be helpful for the forming operation through conical converging dies.

APPENDIX A

Of course, the value of σ_2 (-p) varies over the surface of the work piece. For a particular compression condition the value of σ_2 (-p) is constant when yielding starts. Hence the value of λ is constant during a particular compression condition, although the value of λ varies slightly during successive reduction of the work piece due to the variation of p in each compression condition. It requires an accurate determination of the variation of λ and/or σ_2 (-p) at the die- work piece interface during each reduction. But this consideration will extend the numerical calculations considerably. Considering equation (13) the moment yielding starts, the value of σ_{rr} (or σ_{xx}) is negligible in comparison to p. Hence for all practical purposes σ_{rr} (or σ_{xx}) can be neglected. Hence $p \cong \lambda$. Putting this value of σ_2 (-p) in equation (3) gives the value of λ associated with yielding. Hence equation (3) on simplification reduces to

$$\lambda = \frac{\rho^k \sigma_0}{(1-2\eta)} \quad \text{for axisymmetric compression}$$

List of symbols

τ = Shear stress
μ = Coefficient of friction
k = Constant equal to 2 in yield criterion
n = A constant quantity much greater than 1
λ = Flow stress of metal powder perform
r, θ, ϕ = Spherical co-ordinates
ρ = Relative density of the perform
ρ^*, ρ_r = Densities of apparent and real contact areas
σ_m = Mean yield stress
σ_0 = Yield stress of the non-work hardening matrix metal
$\dot{\varepsilon}_r, \dot{\varepsilon}_\theta, \dot{\varepsilon}_\phi$ = Principal strain increment
η = Constant and a function of ρ only
p = ram pressure
r = Radius of the sticking zone
J_2' = Second invariant of deviatoric stress
R_0 = Initial radius of the rod
R_f = Final radius of the rod
V_0 = Velocity of incoming flow
V_f = Velocity of exiting flow
Δv = Velocity discontinuity
V = Volume of deformation zone
α = semi cone angle of the die
Γ_I = Surface of velocity discontinuity
σ_{xb} = Extrusion stress

REFERENCES

[1] P. Ramakrishnan: Proc. Int. Seminar on Metal Working Technology Today and Tomorrow, Ranchi, India, 1980, 43-46.
[2] A. K Jha and S. Kumar: Int. J. Mach. Tool Des. Res., 1983, **23**, 201-210.
[3] A. K Jha and S. Kumar: Adv. Tech Plast., 1984, **1**, 353-357.
[4] A. K Jha and S. Kumar: J. Inst. Eng. Ind., 1985, **65**, 169-174.
[5] T.Tabata., S.Masaki and K. Hosokawa: Int. J. Powder Metallurgy Powder Tech., 1980, **16**, 149-161.
[6] T. Wonklin: Proc. First WCIT, 1972, Paper No.- F-7.
[7] B. V.Deryagin: Izd. Akad. Nauk, 1952, U.S.S.R.
[8] B. W. Rooks: 15th Int. MTDR Conf., Birmingham, UK, Macmillan, London, 1975, 487-495.
[9] T. Tabata, S. Masaki and Y. Abe: J. Jpn. Soc, Technol. Plast., 1977, **18**, 373-382.
[10] M. Oyane and T. Tabata: J. Jpn. Soc. Plast., 1974, **18**, 373-381